Data Sheet (Cat.No.T1764)

TargetMol

Adezmapimod

Chemical Properties

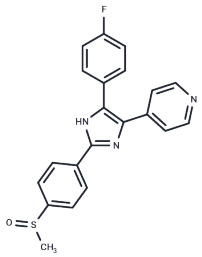

CAS No. : 152121-47-6

Formula: C21H16FN3OS

Molecular Weight: 377.43

Storage: Keep away from direct sunlight
Powder: -20°C for 3 years | In solvent: -80°C for 1 year
Actual storage temperature shall be subject to the COA.

Biological Description

Description	Adezmapimod (SB 203580) is a selective, ATP-competitive p38 MAPK inhibitor (IC50=0.3-0.5 μM) that activates autophagy and mitochondrial autophagy, with more than 100-fold higher selectivity over PKB, LCK, and GSK-3β.
Targets(IC50)	Mitophagy,HSP,Autophagy,p38 MAPK
In vitro	**METHODS**: Human hepatocellular carcinoma cells HepG2 were treated with Adezmapimod (0.1-20 μM) for 30 min, and the expression levels of target proteins were detected by Western Blot. **RESULTS**: Adezmapimod dose-dependently activated ERK but not p38 and JNK, and the maximum activation of ERK was between 1-10 μM. [1] **METHODS**: CD4+ T cells were treated with Adezmapimod (1-25 μM) for 72 h. The proliferation of Tregs was analyzed by Flow Cytometry. **RESULTS**: Adezmapimod inhibited TNF-induced proliferation of Tregs in a dose-dependent manner, with inhibition rates ranging from 32.0-73.2%. Adezmapimod treatment also significantly reduced the proportion of Foxp3+ Tregs in cultured CD4+ T cells, with inhibition rates ranging from 24.9-47.05%. [2]
In vivo	**METHODS**: To examine the in vivo activity, Adezmapimod (25 mg/kg in 4% DMSO+30% PEG 300+5% Tween 80+61% ddH2O) was administered to LPS-treated C57BL/6J mice by a single intraperitoneal injection, and then the mice were killed 24 and 72 h later. **RESULTS**: The LPS-induced up-regulation of Ki-67 and TNFR2 expression on Tregs was completely eliminated by Adezmapimod treatment. The inhibitory effect of Adezmapimod on the proliferation of Tregs in LPS-treated mice lasted for at least 72 h. [2] **METHODS**: To detect the effects on endometriosis (EM) development, Adezmapimod (1 μg/mg) was injected intraperitoneally into EM-induced BALB/c mice once daily for twenty-four days. **RESULTS**: Adezmapimod reduced the weight and size of endometriotic lesions in mice. Levels of IL-1β, TNF-α, MMP-2, and MMP-9 were reduced in peritoneal cells in the Adezmapimod group compared to the EM group. p38 MAPK phosphorylation levels were elevated in the EM group, and Adezmapimod down-regulated phosphorylation levels. [3]
Kinase Assay	Cells were lysed in Buffer A for Western blotting and PKB kinase assays. Kinase assays were performed according to the manufacturer's instructions. Briefly, 4 μg of sheep anti-

Kinase Assay	PKBα was immobilized on 25 μl of protein G-Sepharose overnight (or 1.5 h) and washed in Buffer A (50 mM Tris, pH 7.5, 1 mM EDTA, 1 mMEGTA, 0.5 mM Na3VO4, 0.1% β-mercaptoethanol, 1% Triton X-100, 50 mM sodium fluoride, 5 mM sodium pyrophosphate, 0.1 mM phenylmethylsulfonyl fluoride, 1 μg/ml aprotinin, pepstatin, leupeptin, and 1 μM microcystin). The immobilized anti-PKB was then incubated with 0.5 ml of lysate (from 5 × 10^6 cells) for 1.5 h and washed three times in 0.5 ml of Buffer A supplemented with 0.5 M NaCl, two times in 0.5 ml of Buffer B (50 mM Tris-HCl, pH 7.5, 0.03% (w/v) Brij-35, 0.1 mM EGTA, and 0.1% β-mercaptoethanol), and twice with 100 μl of assay dilution buffer; 5× assay dilution buffer is 100 mM MOPS, pH 7.2, 125 mMβ-glycerophosphate, 25 mM EGTA, 5 mM sodium orthovanadate, 5 mM DTT. To the PKB enzyme immune complex was added 10 μl of assay dilution buffer, 40 μM protein kinase A inhibitor peptide, 100 μM PKB-specific substrate peptide, and 10 μCi of [γ-32P]ATP, all made up in assay dilution buffer. The reaction was incubated for 20 min at room temperature with shaking, then samples were pulse spun, and 40 μl of reaction volume were removed into another tube to which was added 20 μl of 40% trichloroacetic acid to stop the reaction. This was mixed and incubated for 5 min at room temperature, and 40 μl was transferred onto P81 phosphocellulose paper and allowed to bind for 30 s. The P81 pieces were washed three times in 0.75% phosphoric acid then in acetone at room temperature. γ-32P incorporation was then measured by scintillation counting [1].
Cell Research	The luciferase reporter plasmid pIL6luc(-122) and the CAT reporter plasmid p(TRE)5CAT were transfected into TF-1 cell line by means of electroporation. Prior to transfection, cells were cultured for 16?h at a density of 0.5×10^6 cells/ml in the appropriate medium, washed twice and resuspended in RPMI 1640 at a density of 10×10^6 in 200?μl. When transfected with a single plasmid, 25?μg of DNA was added and the mixture was left at room temperature for 15?min. Cotransfections were performed with 15?μg of the reporter plasmid pIL6luc(-122) together with 15?μg of the dominant-negative expression plasmids (pRSV-MKK3(Ala), pcDNA3-MKK6(K82A), pRSV-NΔRaf1, pcDNA3-MKK4(Ala), pcDNA3-Flag-JNK1, or pcDNA3 (empty vector). Cotransfections of pGAL4tkluc (5?μg) with either pGAL4p65 (5?μg) or pGAL4dbd (5?μg) were performed under similar conditions. In addition, cells were cotransfected with 2?μg of a CMV-CAT plasmid, to normalize for transfection efficiency. Electroporation, in 0.4?cm electroporation cuvettes, was performed at 240?V and 960?μF with Gene Pulser electroporator. After electroporation, the cells were replated in RPMI 1640 containing 2% FBS. Six hours after transfection cells were stimulated for 24?h with medium or OA (30?ng/ml) or SB203580 for 30?min prior to OA stimulation. The cells were then harvested and lysed by commercially available luciferase lysis buffer. One-hundred μl of lysis product was added to 100?μl of luciferase assay reagents and luciferase activity was measured with the Anthos Lucy1 luminometer. CAT reporter activity of 100?μl lysis product plus 100?μl CAT dilution buffer was determined with a commercially available CAT Elisa kit [3].
Animal Research	In survival studies, C57BL/6J mice weighing 20 g to 30 g were briefly anesthetized with isoflurane and challenged with 0.05 mL of IT normal saline (NS, noninfected controls) or E. coli (15 × 10^9 CFU/kg) as previously described. One hour before NS challenge, mice (n = 24) received either intraperitoneal SB203580 (100 mg/kg in 0.25 mL) or diluent only (placebo). Infected animals received SB203580 in doses of 100, 10, 1, or 0.1 mg/kg or placebo 1 hour before IT E. coli (n = 241); SB203580 100 or 0.1 mg/kg or placebo 1 hour after E. coli (n = 121); or SB203580 100 mg/kg or placebo 12 hours after E. coli (n = 72). All animals received ceftriaxone (100 mg/kg in 0.1 mL, subcutaneously) for 4 days and NS (0.5 mL, subcutaneously) for 1 day beginning 4 hours after challenge. Animals were observed every 2 hours for the initial 48 hours, every 4 hours from 48 hours to 72 hours, every 8 hours from 72 hours to 96 hours, and then twice daily until study completion (168 hours). Sequential weekly experiments with 24 animals each compared either two to three doses of SB203580 versus placebo administered at similar times or similar

Animal Research	doses of SB203580 versus placebo at differing treatment times. Study groups in each experiment were of equivalent sample size (i.e., 6 – 8 per group) [5].

Solubility Information

Solubility	DMSO: 101 mg/mL (267.6 mM),Sonication is recommended. (< 1 mg/ml refers to the product slightly soluble or insoluble)
In vivo Formulation	10% DMSO+40% PEG300+5% Tween 80+45% Saline: 5 mg/mL (13.25 mM),Solution. *Please add the solvents sequentially, clarifying the solution as much as possible before adding the next one. Dissolve by heating and/or sonication if necessary. Working solution is recommended to be prepared and used immediately. The formulation provided above is for reference purposes only. In vivo formulations may vary and should be modified based on specific experimental conditions.*

Preparing Stock Solutions

	1mg	5mg	10mg
1 mM	2.6495 mL	13.2475 mL	26.495 mL
5 mM	0.5299 mL	2.6495 mL	5.299 mL
10 mM	0.2649 mL	1.3247 mL	2.6495 mL
50 mM	0.053 mL	0.2649 mL	0.5299 mL

Please select the appropriate solvent to prepare the stock solution, according to the solubility of the product in different solvents. Please use it as soon as possible.

Note: The dilution table applies only to solid products. For liquid products, please calculate the stock solution based on the stated concentration and/or density.

Reference

Henklova P, et al. SB203580, a pharmacological inhibitor of p38 MAP kinase transduction pathway activates ERK and JNK MAP kinases in primary cultures of human hepatocytes. Eur J Pharmacol. 2008 Sep 28;593(1-3):16-23.
Zhao Y, Li Y, Zhu R, et al.RPS15 interacted with IGF2BP1 to promote esophageal squamous cell carcinoma development via recognizing m6A modification.Signal Transduction and Targeted Therapy.2023, 8(1): 224.
Shao S, Xia H, Hu M, et al. Isotalatizidine, a C19-diterpenoid alkaloid, attenuates chronic neuropathic pain through stimulating ERK/CREB signaling pathway-mediated microglial dynorphin A expression. Journal of Neuroinflammation. 2020, 17(1): 1-11
Li Z J, Hou Y J, Hao G P, et al. CUDC-907 enhances TRAIL-induced apoptosis through upregulation of DR5 in breast cancer cells. Journal of Cell Communication and Signaling. 2020: 1-11.
Lyu L, Hu Y, Yin S, et al. Autophagy inhibition enhances anti-pituitary adenoma effect of tetrandrine. Phytotherapy Research. 2021, 35(7): 4007-4021.
Zhang H, Wei Q, Gao Z, et al. G protein-coupled receptor 30 mediates meiosis resumption and gap junction communications downregulation in goat cumulus-oocyte complexes by 17β-estradio. Journal of Steroid Biochemistry and Molecular Biology. 2019, 187: 58-67
Hu S, Zhu L, Song Y, et al. Radiation-induced abscopal reproductive effect is driven by TNF-α/p38 MAPK/Rac1 axis in Sertoli cells. Theranostics. 2021 Mar 31;11(12):5742-5758. doi: 10.7150/thno.56853. eCollection 2021.
Zhou B, Yan J, Guo L, et al. Hepatoma cell-intrinsic TLR9 activation induces immune escape through PD-L1 upregulation in hepatocellular carcinoma. Theranostics. 2020, 10(14): 6530.
Li Z J, Hou Y J, Hao G P, et al. CUDC-907 enhances TRAIL-induced apoptosis through upregulation of DR5 in breast cancer cells. Journal of Cell Communication and Signaling. 2020: 1-11.
Cen W J, Feng Y, Li S S, et al. Iron overload induces G1 phase arrest and autophagy in murine preosteoblast cells. Journal of cellular physiology. 2018, 233(9): 6779-6789.
Tang J, Yao C, Liu Y, et al. Arsenic trioxide induces expression of BCL-2 expression via NF-κB and p38 MAPK signaling pathways in BEAS-2B cells during apoptosis. Ecotoxicology and Environmental Safety. 2021, 222: 112531.
Wang D, Wang H, Yan Y, et al.Coating 3D-printed bioceramics with histatin promotes adhesion and osteogenesis of stem cells.Tissue Engineering.2023 (ja).
He T, et al. The p38 MAPK Inhibitor SB203580 Abrogates Tumor Necrosis Factor-Induced Proliferative Expansion of Mouse CD4+Foxp3+ Regulatory T Cells. Front Immunol. 2018 Jul 9;9:1556.
Jiang Y, Zhao X, Chen J, et al.PM2. 5 induces cardiac malformations via PI3K/akt2/mTORC1 signaling pathway in zebrafish larvae.Environmental Pollution.2023: 121306.
Du T, Yan Z, Zhu S, et al. QKI deficiency leads to osteoporosis by promoting RANKL-inducedosteoclastogenesis and disrupting bone metabolism. Cell Death and Disease. 2020
Wen Y, Peng D, Li C, et al. A new polysaccharide isolated from Morchella importuna fruiting bodies and its immunoregulatory mechanism. International Journal of Biological Macromolecules. 2019, 137: 8-19.
Yuan J, Yao C, Tang J, et al. Enhanced GRP78 protein expression via the IRE1α/ASK1/p38 MAPK pathway during As2O3-induced endoplasmic reticulum stress in BEAS-2B cells. Toxicology. 2021, 462: 152962.
Hu Q, Du H, Ma G, et al. Purification, identification and functional characterization of an immunomodulatory protein from Pleurotus eryngii. Food & Function. 2018, 9(7): 3764-3775
Zhu N, Xiang Y, Zhao X, et al. Thymoquinone suppresses platelet-derived growth factor-BB-induced vascular smooth muscle cell proliferation, migration and neointimal formation. Journal of Cellular and Molecular Medicine. 2019
Xie D, Ge X, Ma Y, et al. Clemastine improves hypomyelination in rats with hypoxic-ischemic brain injury by reducing microglia-derived IL-1β via P38 signaling pathway. Journal of neuroinflammation. 2020, 17(1): 1-17.
Liu Y, Tang J, Yuan J, et al. Arsenite-induced downregulation of occludin in mouse lungs and BEAS-2B cells via the ROS/ERK/ELK1/MLCK and ROS/p38 MAPK signaling pathways. Toxicology Letters. 2020, 332: 146-154
Da Q, Yan Z, Li Z, et al. TAK1 is involved in sodium L-lactate-stimulated p38 signaling and promotes apoptosis. Molecular and Cellular Biochemistry. 2020: 1-10
Lu D, Zhang H, Zhang Y, et al. Secreted MbovP0145 Promotes IL-8 Expression through Its Interactive β-Actin and MAPK Activation and Contributes to Neutrophil Migration. Pathogens. 2021, 10(12): 1628.
Zhao M, Zheng Z, Yin Z, et al.DEL-1 deficiency aggravates pressure overload-induced heart failure by promoting

neutrophil infiltration and neutrophil extracellular traps formation.Biochemical Pharmacology.2023: 115912.
Sui A, Yao C, Chen Y, et al.Polystyrene nanoplastics inhibit StAR expression by activating HIF-1α via ERK1/2 MAPK and AKT pathways in TM3 Leydig cells and testicular tissues of mice.Food and Chemical Toxicology.2023: 113634.
Zhou WD, et al. SB203580, a p38 mitogen-activated protein kinase inhibitor, suppresses the development of endometriosis by down-regulating proinflammatory cytokines and proteolytic factors in a mouse model. Hum Reprod. 2010 Dec;25(12):3110-6.
Cui S, Suo N, Yang Y, et al.The aminosteroid U73122 promotes oligodendrocytes generation and myelin formation. Acta Pharmacologica Sinica.2023: 1-12.
Zhang X, Wang J, Wang M, et al.IFN-β Pretreatment Alleviates Allogeneic Renal Tubular Epithelial Cell-Induced NK Cell Responses via the IRF7/HLA-E/NKG2A Axis.The Journal of Immunology.2023
Ni L, Zhu X, Zhao Q, et al.Dihydroartemisinin, a potential PTGS1 inhibitor, potentiated cisplatin-induced cell death in non-small cell lung cancer through activating ROS-mediated multiple signaling pathways.Neoplasia.2024, 51: 100991.
Sun M, Song Y, Hu X, et al.Leptin reduces LPS-induced A1 reactive astrocyte activation and inflammation via inhibiting p38-MAPK signaling pathway.Glia.2024
Kong F, Liu H, Xu T, et al.RG108 attenuates acute kidney injury by inhibiting P38 MAPK/FOS and JNK/JUN pathways. International Immunopharmacology.2024, 142: 113077.
Jin N, et al. The selective p38 mitogen-activated protein kinase inhibitor, SB203580, improves renal disease in MRL/lpr mouse model of systemic lupus. Int Immunopharmacol. 2011 Sep;11(9):1319-26.
Liang Y, Qian Y, Tang J, et al.Arsenic trioxide promotes ERK1/2-mediated phosphorylation and degradation of BIMEL to attenuate apoptosis in BEAS-2B cells.Chemico-Biological Interactions.2022: 110304.
Yu Y, Wu T, Zhang X, et al.Regorafenib activates oxidative stress by inhibiting SELENOS and potentiates oxaliplatin-induced cell death in colon cancer cells.European Journal of Pharmacology.2023: 175986.
Su J, et al. SB203580, a p38 inhibitor, improved cardiac function but worsened lung injury and survival during Escherichia coli pneumonia in mice. J Trauma. 2010 Jun;68(6):1317-27.
Lin X, Wang Y, Guo X, et al.Shikonin promotes rat periodontal bone defect repair and osteogenic differentiation of BMSCs by p38 MAPK pathway.Odontology.2022: 1-9.
Liu J, Lv L, Gong J, et al. Overexpression of F-box only protein 31 predicts poor prognosis and deregulates p38α- and JNK-mediated apoptosis in esophageal squamous cell carcinoma [J]. International journal of cancer. 2018 Jan 1;142(1):145-155.
Zhu Y, Xiao Y, Kong D, et al. Down-Regulation of miR-378d Increased Rab10 Expression to Help Clearance of Mycobacterium tuberculosis in Macrophages. Frontiers in cellular and infection microbiology. 2020, 10: 108.
Chang Y H, Chiang C Y, Fu E, et al. Staphylococcus aureus enhances gelatinase activities in monocytic U937 cells and in human gingival fibroblasts. Journal of Dental Sciences. 2022
Zhou B, Yan J, Guo L, et al. Hepatoma cell-intrinsic TLR9 activation induces immune escape through PD-L1 upregulation in hepatocellular carcinoma[J]. Theranostics. 2020, 10(14): 6530.
Hu S, Zhu L, Song Y, et al. Radiation-induced abscopal reproductive effect is driven by TNF-α/p38 MAPK/Rac1 axis in Sertoli cells[J]. Theranostics. 2021, 11(12): 5742.
Kong L, Huang H, Luan S, et al. Inhibition of ASIC1a-Mediated ERS Improves the Activation of HSCs and Copper Transport Under Copper Load. Frontiers in Pharmacology. 2021, 12: 1348.